Journal of Physics: Conference Series **1610** (2020) 012013 doi:10.1088/1742-6596/1610/1/012013

Double charge exchange reactions as a probe for neutrinoless double beta decay nuclear matrix elements

E. Santopinto[1], J. Ferretti[2], H. García-Tecocoatzi[3], R. Magana Vsevolodovna[1] and within the NUMEN project.

E-mail: elena.santopinto@ge.infn.it
[1] INFN, Sezione di Genova, via Dodecaneso 33, Genova 16146, Italy
[2] Department of Physics, University of Jyväskylä, P.O. Box 35 (YFL), 40014 Jyväskylä, Finland
[3] Department of Physics, University of La Plata (UNLP), 49 y 115 cc. 67, 1900 La Plata, Argentina

Abstract. The formalism to describe heavy-ion double charge exchange (DCE) processes in the eikonal and small-momentum transfer approximations introduced in Phys. Rev. C **98**, 061601(R) (2018) is briefly discussed. It is also shown that, under the previous approximations, the heavy-ion DCE cross-section can be factorized in terms of a reaction and a nuclear part. A double charge exchange effective potential is explicitly derived in the closure approximation and also for the first time the explicit form of the DCE nuclear matrix elements, that are of the form of double Gamow-Teller and double Fermi. The recent hypothesis of a linear correlation between double Gamow-Teller neutrinoless double beta decay and DCE nuclear matrix elements is confirmed thanks to the first explicit derivation of DCE nuclear matrix elements, and by means of microscopic IBM2 calculations.

1. Introduction

Neutrinoless double beta ($0\nu\beta\beta$) decays rank as one of the most interesting Beyond the Standard Model processes. Their experimental observation would imply that the conservation of the lepton number is violated and that the neutrinos are Majorana-type particles. Moreover, it may also provide a mean to measure the neutrino mass. There are several ongoing experimental searches, including EXO [1], Cuore [2], KamLAND-Zen [3] and Gerda [4]. None of them has provided indications of $0\nu\beta\beta$ decays yet.

There have been strong theoretical efforts to provide guidelines to the experimentalists. However, there are strong discrepancies among the results in the different approaches [5, 6, 7, 8, 9, 10]. In particular, the Nuclear Matrix Elements (NMEs) computed within the different nuclear models disagree by more than a factor of two. Furthermore, these results may require additional renormalization or quenching [11]. A possible mean to overcome these difficulties is to use heavy-ion double-charge exchange (DCE) processes to put constraints on neutrinoless $0\nu\beta\beta$ nuclear matrix elements.

Several heavy-ion DCE experiments are ongoing at RNCP Osaka [12, 13], RIBF RIKEN [14], and LNS INFN [15, 16, 17]. The first two of them make use of high-energy heavy-ion double-

charge exchange processes in order to study multi-spin-isospin flip excitation modes, such as a high-energy double Gamow-Teller giant resonance (DGT-GR) [12], that has been predicted three decades ago [18, 19]. The experiment at LNS-INFN is aiming to extract information to put constraints on some of the nuclear matrix elements relevant to $0\nu\beta\beta$ decays [15, 16, 17]. All these experiments have triggered a strong theoretical interest [20, 21, 22, 23], including the effort in the improvement of the reaction part [24, 25, 26].

In the present contribution, we briefly discuss some aspects of the heavy-ion DCE formalism of Ref. [21]. There, for the first time the formalism to describe heavy-ion DCE was explicitly developed by making use of the eikonal approximation.

2. DCE potential

In DCE reactions, two pairs of nucleons – one from the target and one from the projectile – interact. In particular, two protons (neutrons) are converted into two neutrons (protons) in the target, and two neutrons (protons) are converted into two protons (neutrons) in the projectile, with the mass number of the target, A, and the projectile, a, both remaining unchanged. A derivation of a DCE effective potential, describing both long- and short-range interactions, was carried out in Ref. [21] by considering the one-pion-exchange and short-range-interaction diagrams depicted in Fig. 1.

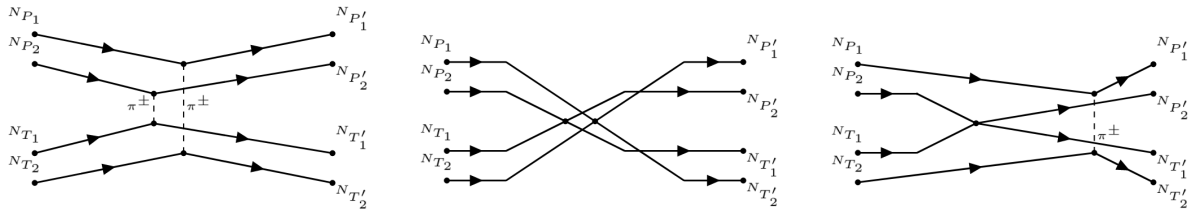

Figure 1. Leading diagrams in a double-charge-exchange process. From left to right, they represent a double-pion-exchange interaction, a double contact term and a mixed one-pion-exchange plus contact term. Figure taken from Ref. [21]; APS CopyRight.

By making use of the closure approximation, which consists in averaging over the intermediate nuclear states [27, 28], one obtains [21]

$$\begin{aligned} V^{\rm DCE}(\vec{q}_1,\vec{q}_2) &= \tfrac{4}{3}\left(\tfrac{f_\pi}{m_\pi}\right)^4 \left(\tfrac{(\vec{\sigma}_{\rm P1}\cdot\vec{q}_1)(\vec{\sigma}_{\rm T1}\cdot\vec{q}_1)}{\omega_1(\omega_1+\bar{E}_{\rm P})}\vec{\tau}_{\rm P1}\cdot\vec{\tau}_{\rm T1}\right)\left(\tfrac{(\vec{\sigma}_{\rm P2}\cdot\vec{q}_2)(\vec{\sigma}_{\rm T2}\cdot\vec{q}_2)}{\omega_2(\omega_2+\bar{E}_{\rm P})(\omega_2+\bar{E}_{\rm T})}\ \vec{\tau}_{\rm P2}\cdot\vec{\tau}_{\rm T2}\right) \\ &+ 2\left[\tfrac{c_{\rm T}^2}{\bar{E}_{\rm P}^{\rm F}+\bar{E}_{\rm T}^{\rm F}} + \tfrac{c_{\rm GT}^2(\vec{\sigma}_{\rm P1}\cdot\vec{\sigma}_{\rm T1})(\vec{\sigma}_{\rm P2}\cdot\vec{\sigma}_{\rm T2})}{\bar{E}_{\rm P}^{\rm GT}+\bar{E}_{\rm T}^{\rm GT}} + \tfrac{c_{\rm T}c_{\rm GT}(\vec{\sigma}_{\rm P2}\cdot\vec{\sigma}_{\rm T2})}{\bar{E}_{\rm P}^{\rm GT}+\bar{E}_{\rm T}^{\rm F}} + \tfrac{c_{\rm T}c_{\rm GT}(\vec{\sigma}_{\rm P1}\cdot\vec{\sigma}_{\rm T1})}{\bar{E}_{\rm P}^{\rm F}+\bar{E}_{\rm T}^{\rm GT}}\right] \\ &\times (\vec{\tau}_{\rm P1}\cdot\vec{\tau}_{\rm T1})(\vec{\tau}_{\rm P2}\cdot\vec{\tau}_{\rm T2}) + \left[\left(\tfrac{f_\pi}{m_\pi}\right)^2\left(\tfrac{(\vec{\sigma}_{\rm P1}\cdot\vec{q}_1)(\vec{\sigma}_{\rm T1}\cdot\vec{q}_1)}{\omega_1(\omega_1+\bar{E}_{\rm P})(\omega_1+\bar{E}_{\rm T})}\ \vec{\tau}_{\rm P1}\cdot\vec{\tau}_{\rm T1}\right)\right. \\ &\times \left.\Big(c_{\rm T}(\vec{\tau}_{\rm P2}\cdot\vec{\tau}_{\rm T2}) + c_{\rm GT}(\vec{\sigma}_{\rm P2}\cdot\vec{\sigma}_2)(\vec{\tau}_{\rm P2}\cdot\vec{\tau}_{\rm T2})\Big) + 1\leftrightarrow 2\right]\ , \end{aligned} \tag{1}$$

where $\left(\frac{f_\pi}{m_\pi}\right)^2 \simeq 400$ MeV·fm^3 [29], the values of the parameters $c_{\rm GT} = 217$ MeV fm^3 and $c_{\rm T} = 151$ MeV fm^3 are taken from the literature [29], and $\omega_i = \sqrt{\vec{q}_i^{\,2}+m_\pi^2}$. The labels P1, P2, T1 and T2 stand for the nucleons within the projectile (P1 and P2) and the target (T1 and T2) involved in the DCE process. The projectile and target closure energies are given by $\bar{E}_{\rm p}^{\alpha} = \langle E_n^a - E_i^a\rangle_\alpha$ and $\bar{E}_{\rm t}^{\alpha} = \langle E_n^A - E_i^A\rangle_\alpha$, respectively, and the superscript α =GT or F, indicates the type of energy excitation. The first line of Eq. (1) corresponds to the double-pion-exchange contribution (first diagram of Fig. 1), the second to the double-contact term (second diagram of Fig. 1), finally the third line to the mixed pion-exchange contact-term (third diagram of Fig. 1).

3. DCE cross-section and microscopic IBM2 nuclear matrix elements

The previous formalism can be used to compute the DCE nuclear matrix elements within the microscopic Interacting Boson Model (IBM2) [30] and the DCE cross-sections in the low-momentum transfer limit by making use of the distorted-wave Born approximation (DWBA).

If one considers transitions between 0^+ and 0^+ ground states, the differential cross section is given by [21]

$$\frac{d\sigma}{d\Omega} = \frac{k}{k'}\left(\frac{\mu}{4\pi^2\hbar^2}\right)^2 |T_{\rm if}|^2 \ , \tag{2}$$

where μ is the reduced mass of the target-projectile system, k and k' are the incoming and outgoing momenta, and $T_{\rm if}$ is the T-matrix of the reaction. $T_{\rm if}$ can be calculated by means of the Distorted Wave Born Approximation (DWBA),

$$T_{\rm if} = \left\langle \Psi^-_{\vec{k}'}\Phi_{\rm f}\right| V \left|\Psi^+_{\vec{k}}\Phi_{\rm i}\right\rangle = \frac{1}{(2\pi)^{3/2}}\int d\vec{R}\ {\rm e}^{i\left(\chi(b)-\vec{Q}\cdot\vec{R}\right)} M_{\rm if}(\vec{m}) \ , \tag{3}$$

where one also uses the eikonal approximation for the c.m. scattering. In the previous equation, $\Psi^+_{\vec{k},\vec{k}'}$ are the wave functions which describe the c.m. motion of the target and projectile ions, $\Phi_{\rm i,f}$ the intrinsic wave functions of the nuclei before and after the interaction, which can be written as the product of projectile and target nucleon wave functions. In the particular case of $0^+_{\rm i} \to 0^+_{\rm f}$ transitions of the target, one gets [21]

$$M_{\rm if}(\mathbf{m}) \to 2\left[\left(\frac{\mathcal{M}^{\rm DGT}_{\rm T\to T'}\mathcal{M}^{\rm DGT}_{\rm P\to P'}}{\bar{E}^{\rm GT}_{\rm P}+\bar{E}^{\rm GT}_{\rm T}}\right)+\left(\frac{\mathcal{M}^{\rm DF}_{\rm T\to T'}\ \mathcal{M}^{\rm DF}_{\rm P\to P'}}{\bar{E}^{\rm F}_{\rm P}+\bar{E}^{\rm F}_{\rm T}}\right)\right] \ , \tag{4}$$

where $\mathcal{M}^{\rm DGT}$ and $\mathcal{M}^{\rm DF}$ are Double-Gamow-Teller (DGT) and Double-Fermi (DF) nuclear matrix elements, respectively, of the projectile/target (A = P, T). The previous matrix elements are defined as [21]

$$\mathcal{M}^{\rm DGT}_{\rm A\to A'} = c_{\rm GT}\left\langle \Phi^{(\rm A')}_{J'}\right| \sum_{n,n'}[\vec{\sigma}_n\times\vec{\sigma}_{n'}]^{(0)}\vec{\tau}_n\vec{\tau}_{n'}\left|\Phi^{(\rm A)}_{J}\right\rangle \tag{5}$$

and

$$\mathcal{M}^{\rm DF}_{\rm A\to A'} = c_{\rm t}\left\langle \Phi^{(\rm A')}_{J'}\right| \sum_{n,n'}\vec{\tau}_n\vec{\tau}_{n'}\left|\Phi^{(\rm A)}_{J}\right\rangle \ , \tag{6}$$

where the sum runs over the nucleons (n, n') involved in the process. They are calculated in the microscopic Interacting Boson Model (IBM2) [21, 30]. Finally, the cross section of Eq. (2) can be written in the eikonal approximation and low-momentum transfer limit as

$$\frac{d\sigma}{d\Omega} \to \frac{k}{k'}\left(\frac{\mu}{4\pi^2\hbar^2}\right)^2 \left|2F(\theta)\left(\frac{\mathcal{M}^{\rm DGT}_{\rm T\to T'}\mathcal{M}^{\rm DGT}_{\rm P\to P'}}{\bar{E}^{\rm GT}_{\rm P}+\bar{E}^{\rm GT}_{\rm T}} + \frac{\mathcal{M}^{\rm DF}_{\rm T\to T'}\ \mathcal{M}^{\rm DF}_{\rm P\to P'}}{\bar{E}^{\rm F}_{\rm P}+\bar{E}^{\rm F}_{\rm T}}\right)\right|^2 \ , \tag{7}$$

where $F(\theta)$ is an angular distribution [21, Eq. (14)].

4. Linear correlation between DCE and $0\nu\beta\beta$ nuclear matrix elements

In Ref. [20], the authors discussed the possible emergence of a linear correlation between DGT DCE and $0\nu\beta\beta$ nuclear matrix elements by means of a large-scale shell-model calculation. In Ref. [21], the previous hypothesis was confirmed by making use of a different nuclear model, the microscopic IBM2. Moreover, as also discussed in the previous sections, the existence of a procedure to factorize the DCE cross sections in terms of reaction and nuclear parts was explicitly

demonstrated in the eikonal approximation. Most important, a microscopic description of DCE processes was developed with the derivation of a DCE potential in the closure approximation [21]. Thanks to this, one may think to use the present and forthcoming experimental data of heavy-ion DCE cross-sections to place an upper limit on $0\nu\beta\beta$ NMEs in terms of the DCE experimental data at very forward angles, whereas in the case of larger scattering angles, the nuclear part is expected to be a convolution of beam and target NMEs.

The emergence of the linear correlation between DCE and $0\nu\beta\beta$ nuclear matrix elements can be shown by calculating the previous DCE and $0\nu\beta\beta$ NMEs within the same nuclear model and for a sufficiently large set of nuclei. Then, a simple linear regression analysis can be conducted and a regression line can be drawn. If one plots the microscopic IBM2 results [21, 31] for the ^{116}Cd $\rightarrow$ ^{116}Sn, ^{128}Te $\rightarrow$ ^{128}Xe, ^{82}Se $\rightarrow$ ^{82}Kr, and ^{76}Ge $\rightarrow$ ^{76}Se DGT DCE and $0\nu\beta\beta$ NMEs, one obtains the clear regression line shown in Fig. 2.

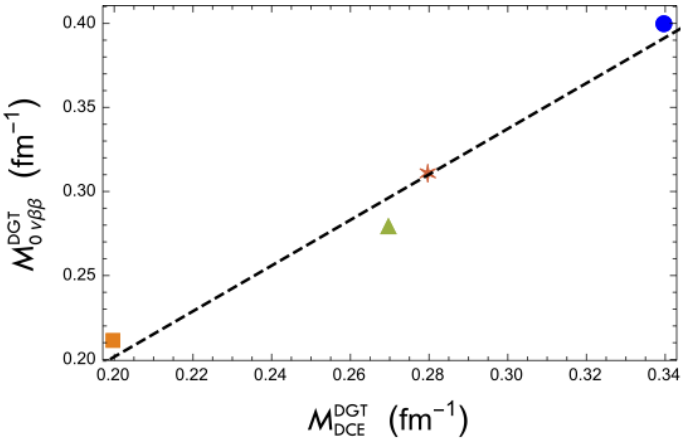

Figure 2. Correlation between calculated DCE-DGT NMEs [21] and $0\nu\beta\beta$-DGT NMEs [31]. The orange square, green triangle, red star, and blue circle stand for ^{116}Cd $\rightarrow$ ^{116}Sn, ^{128}Te $\rightarrow$ ^{128}Xe, ^{82}Se$\rightarrow$ ^{82}Kr and ^{76}Ge $\rightarrow$ ^{76}Se data, respectively. Figure from Ref. [21]; APS CopyRight.

Finally, it is worth to note that the slopes of our curves in Fig. 2 and [21, Figs. 3] and of those reported in [20, Figs. 4] are quite different. The main reason for this mismatch resides in the procedures used in Ref. [20] and [21] to extract the form of the DCE potential, which is needed to calculate the DCE NMEs. In the first case, the authors did not derive the DCE matrix elements explicitly, but they made a guess on the form only of the DGT DCE nuclear matrix elements ; see [20, Eq. (6)]. In the second case, the authors derived the DCE potential of Eq. (1) and [21, Eq. (3)] explicitly from the diagrams of Figs. 1. Because of this, in the results of [20, Figs. 4] one can appreciate the emergence of a linear correlation between DGT DCE and $0\nu\beta\beta$ nuclear matrix elements, but the slopes of the curves are "random". On the contrary, the slopes of the curves in Fig. 2 and [21, Figs. 3] are the "physical" ones.

5. Conclusion

The formalism to calculate the cross-sections and Nuclear Matrix Elements (NMEs) of heavy-ion Double Charge Exchange (DCE) processes of Ref. [21] was briefly described. It was also shown that the heavy-ion DCE cross-section can be factorized in terms of a reaction and a nuclear part and that there is a linear correlation between DCE NME's and neutrinoless NME's [21]. This will make it possible to extract the $0\nu\beta\beta$ NMEs from experimental measurements of DCE cross-sections.

The next step will be to compute the spectroscopic amplitudes and radial transition densities in the microscopic IBM scheme. This will open the possibility to give predictions with microscopic IBM models in the field of charge exchange reactions.

[1] J. B. Albert *et al.* (EXO-200 Collaboration), Nature **510**, 229 (2014).
[2] K. Alfonso *et al.* (CUORE Collaboration), Phys. Rev. Lett. **115**, 102502 (2015).
[3] A. Gando *et al.* (KamLAND-Zen Collaboration), Phys. Rev. Lett. **117**, 082503 (2016).
[4] M. Agostini *et al.* (GERDA Collaboration), Nature **544**, 47 (2017).
[5] J. Suhonen and O. Civitarese, Nucl. Phys. A **847**, 207 (2010).
[6] A. Meroni, S. T. Petcov and F. Šimkovic, JHEP **1302**, 025 (2013).
[7] R. A. Sen'kov and M. Horoi, Phys. Rev. C **88**, 064312 (2013).
[8] F. Šimkovic, V. Rodin, A. Faessler and P. Vogel, Phys. Rev. C **87**, 045501 (2013).
[9] M. T. Mustonen and J. Engel, Phys. Rev. C **87**, 064302 (2013).
[10] J. Barea, J. Kotila and F. Iachello, Phys. Rev. C **91**, 034304 (2015).
[11] J. Engel and J. Menéndez, Rept. Prog. Phys. **80**, 046301 (2017).
[12] M. Takaki *et al.*, JPS Conf. Proc. **6**, 020038 (2015).
[13] M. Takaki *et al.*, CNS Ann. Rep. **94**, 9 (2014).
[14] T. Uesaka *et al.*, RIKEN RIBF NP-PAC, NP1512-RIBF141 (2015).
[15] F. Cappuzzello *et al.*, EPJ Web Conf. **117**, 10003 (2016).
[16] F. Cappuzzello, M. Cavallaro, C. Agodi, M. Bondi, D. Carbone, A. Cunsolo and A. Foti, Eur. Phys. J. A **51**, 145 (2015).
[17] F. Cappuzzello *et al.*, Eur. Phys. J. A **54**, 72 (2018).
[18] P. Vogel, M. Ericson, and J. D. Vergados, Phys. Lett. B**212**, 259 (1988).
[19] N. Auerbach, L. Zamick, and D. C. Zheng, Ann. Phys. (N.Y.) **192**, 77 (1989).
[20] N. Shimizu, J. Menéndez and K. Yako, Phys. Rev. Lett. **120**, 142502 (2018).
[21] E. Santopinto, H. García-Tecocoatzi, R.I. Magaña Vsevolodovna and J. Ferretti, Phys. Rev. C **98**, 061601 (R) (2018).
[22] V. dos S. Ferreira, A. R. Samana, F. Krmpotić and M. Chiapparini, Phys. Rev. C **101**, 044314 (2020).
[23] J. I. Bellone, S. Burrello, M. Colonna, J. A. Lay and H. Lenske, Phys. Lett. B **807**,135528 (2020).
[24] H. Lenske, J. I. Bellone, M. Colonna, and J. A. Lay, Phys. Rev. C **98**, 044620 (2018); H. Lenske, J. Phys. Conf. Ser. **1056**, 012030 (2018).
[25] J. I. Bellone, M. Colonna, H. Lenske and J. A. Lay, J. Phys. Conf. Ser. **1056**, 012004 (2018).
[26] H. Lenske, F. Cappuzzello, M. Cavallaro and M. Colonna, Prog. Part. Nucl. Phys. **109**, 103716 (2019).
[27] W. C. Haxton and G. J. Stephenson, Prog. Part. Nucl. Phys. **12**, 409 (1984).
[28] S. M. Bilenky and C. Giunti, Int. J. Mod. Phys. A **30**, 1530001 (2015).
[29] G. F. Bertsch and H. Esbensen, Rep. Prog. Phys. **50**, 607 (1987).
[30] A. Arima, T. Ohtsuka, F. Iachello and I. Talmi, Phys. Lett. **66B**, 205 (1977).
[31] J. Barea, J. Kotila and F. Iachello, Phys. Rev. C **87**, 014315 (2013).